Immunoblots and immunostaining

Muscles were rapidly homogenized in 1 ml extraction buffer (75 mM Tris-HCl, pH 6.8, 3.8% SDS, 4 M urea, 20% glycerol and 5% β-mercaptoethanol). After protein denaturation (95 °C for 5 min), non-dissolved protein was removed by centrifugation (14,000*g* for 5 min). Fifty micrograms of protein, as determined by Lowry protein assay, was loaded onto each lane, separated on 3–12% SDS–polyacrylamide gel electrophoresis (PAGE) and immunoblotted. For immunostaining, muscles were immediately immersed in optimal cutting temperature compound (OCT; Sakura Finetek) and frozen in liquid-nitrogen-cooled isopentane. Frozen sections (10-μm thick) were incubated with blocking solution (2% horse serum, 1% BSA, 0.5% Triton X-100 in PBS) for 30 min. Primary antibodies were diluted in incubation buffer (2% horse serum, 1% BSA, 0.01% Triton X-100 in PBS) and incubated overnight at 4 °C. Sections were washed four times with incubation buffer and appropriate secondary antibodies were incubated at room temperature for 2 h. To determine protein expression levels, the primary antibodies were diluted such that the signal was not saturated. Images were collected and analysed with a confocal microscope (Leica TCS-8P) and appropriate software. The microscope was calibrated using the InSpeck Microscope Image Intensity Calibration Kit (Molecular Probes). Specific intensity was calculated for each image as the signal intensity of the muscle circumference minus that of an adjacent, non-stained region[30]. Five different pictures were taken using the same parameters on each section, and four different sections were used for each individual mouse.

Electron microscopy

Mice were perfused with 2.5% glutaraldehyde in 0.1 M sodium phosphate, pH 7.4. Muscles were post-fixed overnight at 4 °C in 2.5% glutaraldehyde in 0.1 M sodium phosphate. After treatment with 1% OsO_4 in 0.1 M cacodylate buffer (pH 7.2) muscle pieces were rinsed in 1% Na_2SO_4 in 0.1 M cacodylate buffer and imbedded in Epon. Sections (60-nm thick) were cut on a microtome (Ultracut E; Leica) and post-stained with uranyl acetate and lead citrate. The specimens were examined with an electron microscope (Philips EM400) at an accelerating voltage of 80 kV. We took pictures without knowing the genotype of the mice.

Lectin precipitation

Muscles were homogenized in 500 μl incubation buffer (50 mM Tris-HCl, pH 7.5, 0.2 M NaCl, 1.25 mM $CaCl_2$, 1 mM $MgCl_2$). After centrifugation at 20,000*g*, the supernatant was collected and the pellet was re-extracted with 1% Triton X-100 in incubation buffer for 30 min on ice. After centrifugation at 20,000*g*, the supernatant was collected and pooled with the supernatant from the first centrifugation. One hundred microlitres of wheat germ lectin (WGL) Sepharose beads (Amersham Pharmacia) was added and incubated for 2 h at 4 °C. WGL beads were washed four times with incubation buffer and proteins were eluted in 75 mM Tris-HCl, pH 6.8, 3.8% SDS, 4 M urea, 20% glycerol and 5% β-mercaptoethanol. Proteins were separated on 3–12% SDS–PAGE and immunoblotted using anti-chick agrin antibodies.

Received 5 March; accepted 23 July 2001.

1. Tome, F. M. S., Guicheney, P. & Fardeau, M. in *Neuromuscular Disorders: Clinical and Molecular Genetics* (ed. Emery, A. E. H.) 21–57 (John Wiley & Sons, West Sussex, 1998).
2. Miyagoe-Suzuki, Y., Nakagawa, M. & Takeda, S. Merosin and congenital muscular dystrophy. *Microsc. Res. Tech.* **48,** 181–191 (2000).
3. Colognato, H. & Yurchenco, P. D. Form and function: the laminin family of heterotrimers. *Dev. Dyn.* **218,** 213–234 (2000).
4. Campbell, K. P. Three muscular dystrophies: loss of cytoskeleton-extracellular matrix linkage. *Cell* **80,** 675–679 (1995).
5. Mayer, U. *et al.* Absence of integrin α7 causes a novel form of muscular dystrophy. *Nature Genet.* **17,** 318–323 (1997).
6. Ruegg, M. A. & Bixby, J. L. Agrin orchestrates synaptic differentiation at the vertebrate neuromuscular junction. *Trends Neurosci.* **21,** 22–27 (1998).
7. Denzer, A. J., Brandenberger, R., Gesemann, M., Chiquet, M. & Ruegg, M. A. Agrin binds to the nerve-muscle basal lamina via laminin. *J. Cell Biol.* **137,** 671–683 (1997).
8. Gesemann, M., Brancaccio, A., Schumacher, B. & Ruegg, M. A. Agrin is a high-affinity binding protein of dystroglycan in non-muscle tissue. *J. Biol. Chem.* **273,** 600–605 (1998).
9. Patton, B. L., Miner, J. H., Chiu, A. Y. & Sanes, J. R. Distribution and function of laminins in the neuromuscular system of developing, adult, and mutant mice. *J. Cell Biol.* **139,** 1507–1521 (1997).
10. Ringelmann, B. *et al.* Expression of laminin α1, α2, α4, and α5 chains, fibronectin, and tenascin-C in skeletal muscle of dystrophic 129ReJ dy/dy mice. *Exp. Cell Res.* **246,** 165–182 (1999).
11. Talts, J. F. *et al.* Structural and functional analysis of the recombinant G domain of the laminin α 4 chain and its proteolytic processing in tissues. *J. Biol. Chem.* **275,** 35192–35199 (2000).
12. Denzer, A. J. *et al.* Electron microscopic structure of agrin and mapping of its binding site in laminin-1. *EMBO J.* **17,** 335–343 (1998).
13. Burgess, R. W., Nguyen, Q. T., Son, Y. J., Lichtman, J. W. & Sanes, J. R. Alternatively spliced isoforms of nerve- and muscle-derived agrin: their roles at the neuromuscular junction. *Neuron* **23,** 33–44 (1999).
14. Jaynes, J. B., Chamberlain, J. S., Buskin, J. N., Johnson, J. E. & Hauschka, S. D. Transcriptional regulation of the muscle creatine kinase gene and regulated expression in transfected mouse myoblasts. *Mol. Cell. Biol.* **6,** 2855–2864 (1986).
15. Sternberg, E. A. *et al.* Identification of upstream and intragenic regulatory elements that confer cell-type-restricted and differentiation-specific expression on the muscle creatine kinase gene. *Mol. Cell. Biol.* **8,** 2896–2909 (1988).
16. Kuang, W. *et al.* Merosin-deficient congenital muscular dystrophy. Partial genetic correction in two mouse models. *J. Clin. Invest.* **102,** 844–852 (1998).
17. Sunada, Y., Bernier, S. M., Kozak, C. A., Yamada, Y. & Campbell, K. P. Deficiency of merosin in dystrophic dy mice and genetic linkage of laminin M chain gene to dy locus. *J. Biol. Chem.* **269,** 13729–13732 (1994).
18. Xu, H., Wu, X. R., Wewer, U. M. & Engvall, E. Murine muscular dystrophy caused by a mutation in the laminin alpha 2 (Lama2) gene. *Nature Genet.* **8,** 297–302 (1994).
19. Xu, H., Christmas, P., Wu, X. R., Wewer, U. M. & Engvall, E. Defective muscle basement membrane and lack of M-laminin in the dystrophic dy/dy mouse. *Proc. Natl Acad. Sci. USA* **91,** 5572–5576 (1994).
20. Colognato, H. & Yurchenco, P. D. The laminin α2 expressed by dystrophic dy(2J) mice is defective in its ability to form polymers. *Curr. Biol.* **9,** 1327–1330 (1999).
21. MacPike, A. D. & Meier, H. Comparison of dy and dy2J, two alleles expressing forms of muscular dystrophy in the mouse. *Proc. Soc. Exp. Biol. Med.* **151,** 670–672 (1976).
22. Ibraghimov-Beskrovnaya, O. *et al.* Primary structure of dystrophin-associated glycoproteins linking dystrophin to the extracellular matrix. *Nature* **355,** 696–702 (1992).
23. Ervasti, J. M., Kahl, S. D. & Campbell, K. P. Purification of dystrophin from skeletal muscle. *J. Biol. Chem.* **266,** 9161–9165 (1991).
24. Henry, M. D. & Campbell, K. P. A role for dystroglycan in basement membrane assembly. *Cell* **95,** 859–870 (1998).
25. Cote, P. D., Moukhles, H., Lindenbaum, M. & Carbonetto, S. Chimaeric mice deficient in dystroglycans develop muscular dystrophy and have disrupted myoneural synapses. *Nature Genet.* **23,** 338–342 (1999).
26. Meier, T. *et al.* A minigene of neural agrin encoding the laminin-binding and acetylcholine receptor-aggregating domains is sufficient to induce postsynaptic differentiation in muscle fibres. *Eur. J. Neurosci.* **10,** 3141–3152 (1998).
27. Sorokin, L. M., Pausch, F., Durbeej, M. & Ekblom, P. Differential expression of five laminin alpha (1-5) chains in developing and adult mouse kidney. *Dev. Dyn.* **210,** 446–462 (1997).
28. Schulze, B., Mann, K., Battistutta, R., Wiedemann, H. & Timpl, R. Structural properties of recombinant domain III-3 of perlecan containing a globular domain inserted into an epidermal-growth-factor-like motif. *Eur. J. Biochem.* **231,** 551–556 (1995).
29. Herrmann, R. *et al.* Dissociation of the dystroglycan complex in caveolin-3-deficient limb girdle muscular dystrophy. *Hum. Mol. Genet.* **9,** 2335–2340 (2000).
30. Turney, S. G., Culican, S. M. & Lichtman, J. W. A quantitative fluorescence-imaging technique for studying acetylcholine receptor turnover at neuromuscular junctions in living animals. *J. Neurosci. Methods* **64,** 199–208 (1996).

Acknowledgements

We are grateful to M. Chiquet, S. Kröger, U. Mayer, L. Sorokin and R. Timpl for providing us with antibodies. We thank S. Arber, A. Brancaccio and T. Meier for discussions. M. Dürrenberger and U. Sauder for help in electron microscopy; J.-F. Spetz for DNA injection; M. Willem for providing us with the MCK promoter; and P. Scotton for the help with artwork. Special thanks go to D. Walz for his help in the statistical analysis of the results. This work was supported by grants from the Swiss National Science Foundation (MAR), the Kanton of Basel-Stadt (MAR), the Swiss Foundation for Research on Muscle Diseases (MAR and UM), from the National Institutes of Health (EE), the Novartis Research Foundation (UM), the Deutsche Forschungsgemeinschaft, Aktion Benni and company, and the Ernst und Berta Grimmke-Stiftung (HL).

Correspondence and requests for materials should be addressed to M.A.R. (e-mail: markus-a.ruegg@unibas.ch).

Intercellular movement of the putative transcription factor SHR in root patterning

Keiji Nakajima*, Giovanni Sena, Tal Nawy & Philip N. Benfey

Department of Biology, New York University, 1009 Main Building, 100 Washington Square East, New York, New York 10003, USA

Positional information is pivotal for establishing developmental patterning in plants[1–3], but little is known about the underlying signalling mechanisms. The *Arabidopsis* root radial pattern is generated through stereotyped division of initial cells and the subsequent acquisition of cell fate[4]. *short-root* (*shr*) mutants do not undergo the longitudinal cell division of the cortex/endodermis initial daughter cell, resulting in a single cell layer with only cortex attributes[5,6]. Thus, *SHR* is necessary for both cell division and endodermis specification[5,6]. *SHR* messenger RNA is found exclusively in the stele cells internal to the endodermis and cortex, indicating that it has a non-cell-autonomous mode of action[6].

* Present address: Graduate School of Biological Sciences, Nara Institute of Science and Technology, 8916-5 Takayama, Ikoma, Nara 630-0101, Japan.

Here we show that the SHR protein, a putative transcription factor, moves from the stele to a single layer of adjacent cells, where it enters the nucleus. Ectopic expression of *SHR* driven by the promoter of the downstream gene *SCARECROW* (*SCR*) results in autocatalytic reinforcement of SHR signalling, producing altered cell fates and multiplication of cell layers. These results support a model in which SHR protein acts both as a signal from the stele and as an activator of endodermal cell fate and SCR-mediated cell division.

To determine whether SHR protein could move between cells, we fused in-frame the coding regions of SHR and green fluorescent protein (GFP) under the control of the 2.5-kilobase (kb) 5′-upstream region of *SHR*. This promoter element confers an expression pattern that matches the localization of *SHR* mRNA[6] (Fig. 1b, insert). Transforming the *shr-2* mutant (a presumed null allele[6]) with the fusion construct resulted in rescue of the root radial pattern (Fig. 1b) with appropriate cell-fate specification (data not shown), indicating that the fusion protein retained the SHR activity necessary for root patterning.

We analysed the localization of SHR::GFP fluorescence by both confocal and multi-photon laser-scanning microscopy. GFP fluorescence was found not only in the stele, but also in all cells immediately adjacent to the stele (Fig. 1b). These include the quiescent centre (QC), the cortex/endodermis initial and daughter cells, as well as all cells of the endodermis (Fig. 1a) (we refer to these cells collectively as the 'adjacent layer'). *SHR* transcripts have never been detected in any of these cells either by *in situ* hybridization[6] or indirectly through *SHR* promoter reporter gene fusions[6] (Fig. 1b, insert). From the confocal images, it appeared that although GFP fluorescence was localized to both the nuclei and the cytoplasm in the stele, it was primarily localized to the nuclei in the adjacent layer (Fig. 1b). This was confirmed with multi-photon microscopy (Fig. 1c). At the limit of resolution of multi-photon imaging, we could not detect GFP in cortex or epidermal cells, nor in any other organelles or subcellular structures besides the nuclei in endodermal cells (Fig. 1c).

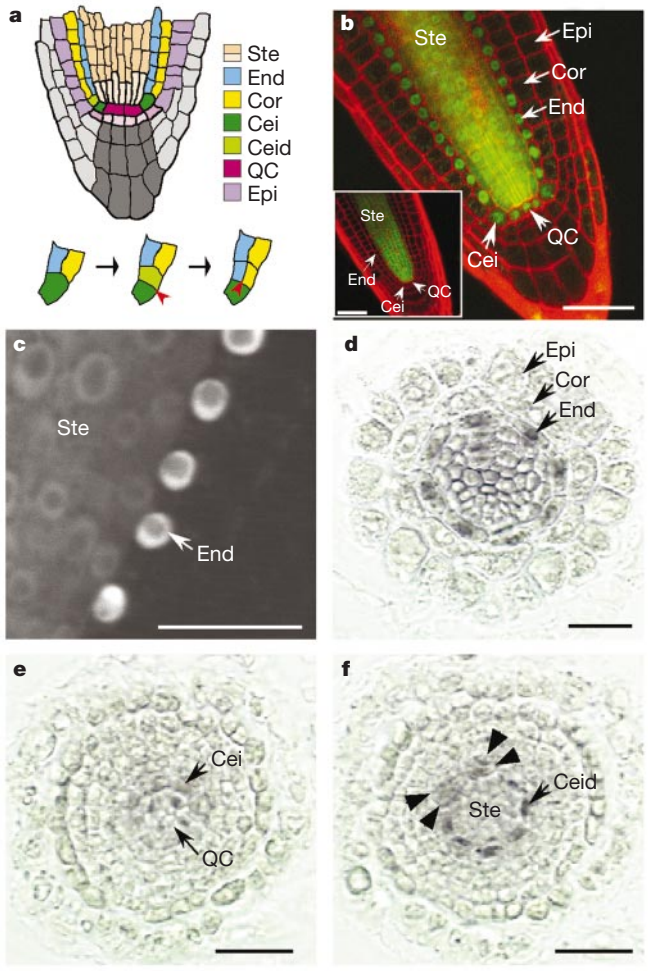

Figure 1 SHR protein localization. **a**, Diagram of *Arabidopsis* root tip and cell divisions (red arrowheads) that form endodermis and cortex. **b**, **c**, Confocal (**b**) and multiphoton (**c**) images of the SHR::GFP transgenic roots (insert in **b**, transcriptional fusion[6]). **d**–**f**, SHR immunostaining on transverse root sections above root meristem (**d**), at the level of the QC (**e**) and Ceid after longitudinal division (**f**). Arrowheads in **f** indicate SHR protein in two Ceid daughters. Cei, cortex/endodermis initial; Ceid, daughter of Cei; Cor, cortex; End, endodermis; Epi, epidermis; Ste, stele; QC, quiescent centre. Scales bars, 50 μm (**b**), 25 μm (**c**–**f**).

To confirm this localization of SHR protein, we produced affinity-purified antibodies to recombinant SHR protein. The specificity of the antibody was analysed on *shr-2* mutant roots where no binding was detected (Supplementary Information Fig. 1b). On transverse sections from just above the root meristem, the antibodies consistently decorated nuclei of endodermal cells (Fig. 1d). In the stele, there was more uniform binding of the antibodies (Fig. 1d), with occasional stronger staining observed in nuclei (Supplementary Information Fig. 1a). In sections at the level of the QC, nuclear localized SHR protein was evident in the four QC cells, as well as in the eight surrounding cortex/endodermis initial cells (Fig. 1e). In the next serial section, strong staining was detected in the initial daughter cells after their longitudinal cell division (Fig. 1f).

Notably, in two of the eight pairs of daughter cells SHR was localized in both nuclei resulting from the longitudinal division (Fig. 1f, triangles), whereas in the remaining six pairs only the inner nucleus appears to contain SHR protein (Fig. 1f). This is probably due to the non-synchronous division of these cells, which results in slightly different times after division being analysed in the pairs of nuclei. Together, these results indicate that SHR is equally partitioned into the two daughter nuclei after the longitudinal cell division, but SHR levels are maintained only in the nucleus of the inner cell.

The simplest explanation for the difference in localization patterns of *SHR* mRNA and protein is movement of SHR protein from the stele to the adjacent layer. An alternative hypothesis is an abnormally rapid degradation of *SHR* mRNA transcribed in or transported to the adjacent layer. We have shown, however, that when *SHR* is driven by the constitutive cauliflower mosaic virus 35S (CaMV35S) promoter, high levels of *SHR* mRNA accumulate in cells outside the stele[6]. Moreover, both the rapid loss of SHR immunostaining in outer daughter cells of the longitudinal division (Fig. 1f) and the lack of GFP fluorescence in the first cell of the cortex lineage in the SHR::GFP lines (Fig. 1b) indicate that SHR protein has a relatively short half-life. Thus, the discrepancy between the mRNA and protein localization is not due to the protein having a much lower turnover rate than the mRNA. We therefore conclude that SHR protein moves from the stele to the single adjacent layer.

To understand better the role of SHR protein in specifying cell fate and mediating cell division in the root, we generated transgenic plants in which *SHR* is transcribed in the adjacent layer. The 2.5-kb *SCR* promoter, which confers expression in all cells of the adjacent layer[6,7], was fused to the full-length *SHR* coding region (*SCRpro::SHR*). This construct was introduced into wild-type plants either with or without a *SCRpro::GFP* reporter. Thirteen independent lines showed an increased number of cell layers in the root (Fig. 2a, b). The supernumerary cell layers exhibited a high degree of radial symmetry. This is in contrast to a phenotype obtained with ectopic *SHR* expression by the CaMV35S promoter,

which displayed fairly chaotic division patterns[6].

The differentiation status of root cells in the *SCRpro::SHR* lines was initially analysed with two monoclonal antibodies specific to epitopes found in the different cell layers: the JIM13 antibody recognizes an arabinogalactan epitope on the endodermis and on some stele cells[8] (Supplementary Information Fig. 2b), and the CCRC-M2 antibody recognizes a carbohydrate epitope in cortex and epidermis cell walls[9] (Supplementary Information Fig. 2c). JIM13 stained all the cell layers except the outermost layer, indicating the presence of endodermal characters in these cells (Fig. 2c). In the outermost layer a few cells were occasionally stained with JIM13. When the same section was treated with CCRC-M2, only the outermost layer was stained (Fig. 2d). Notably, the JIM13-stained cells in the outermost layer were not stained by the CCRC-M2 antibody (Fig. 2c and d, asterisks), suggesting that endodermal specification can override cortex and/or epidermal specification. Acquisition of endodermal characters in the supernumerary layers was confirmed by histochemical staining for the Casparian strip, a cell wall deposit of hydrophobic carbohydrate that occurs specifically in the endodermis[10] (Supplementary Information Fig. 2a). Staining of the Casparian strip was detected in most, if not all, of the cells between the stele and the outermost cell layer (Fig. 2e).

Because SHR protein seems to move not only to the endodermis but also to the QC, we determined the status of QC cells in the *SCRpro::SHR* lines. A GFP marker line, QC433, that exhibits highly specific expression in the QC (Fig. 2f, insert) was crossed to a strong *SCRpro::SHR* line. The F_1 plants had an increased number of GFP-expressing cells as compared with wild-type roots (Fig. 2f). These cells were organized into supernumerary layers between the stele and the root cap. The supernumerary endodermis layers appear to converge on these GFP-expressing cells (Fig. 2f). Crosses to root-cap-specific marker lines indicated that neither the lateral root cap nor the columella root cap was affected in the transgenic roots (data not shown).

To determine whether the cell-fate changes observed in the *SCRpro::SHR* lines correlated with the presence of SHR protein we performed immunolocalization with the anti-SHR antibodies in backgrounds that contained tissue-specific reporters. We crossed a strong *SCRpro::SHR* line with the marker lines, End195 (ref. 11), GL2pro::GUS (ref. 12) and QC46 (ref. 13), which show specific β-glucuronidase (GUS) expression in endodermis, non-hair epidermal cells and QC cells, respectively. The roots of plants from each cross were first stained for GUS activity, and then fixed, sectioned and processed for SHR immunolocalization. Consistent with the

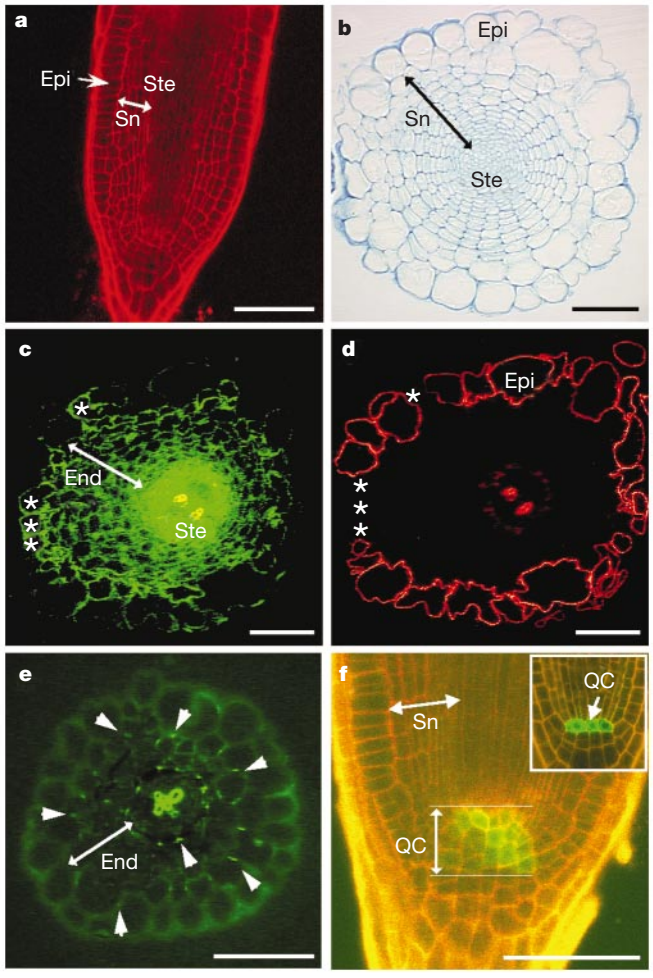

Figure 2 Analysis of *SCRpro::SHR* transgenic roots. **a**, **b**, Confocal image (**a**) and transverse section (**b**) of the *SCRpro::SHR* transgenic root. **c**–**f**, Marker analysis of the *SCRpro::SHR* root. **c**, **d**, JIM13 (**c**) and CCRC-M2 (**d**) antibody stains of the same section. Asterisks indicate the same cells in **c** and **d**. **e**, Casparian strip stain. **f**, Confocal images of the QC433 QC-specific GFP marker (inset, wild type). Sn, supernumerary layers. Other abbreviations as in Fig. 1. Scale bars, 50 μm.

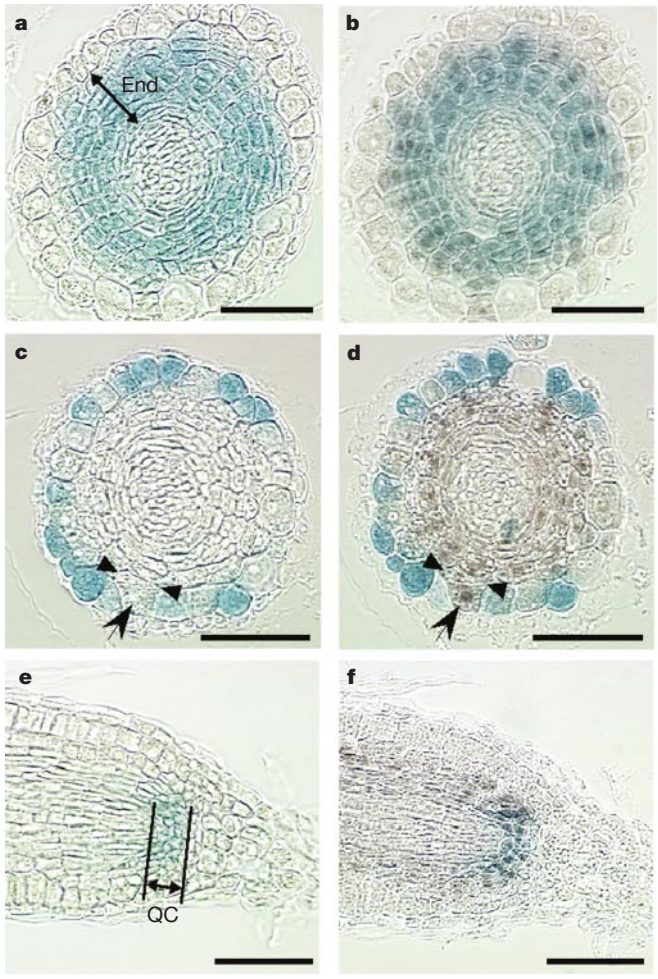

Figure 3 Correlation between the presence of SHR protein and cell fates in *SCRpro::SHR* roots. GUS-stained sections of the crosses between *SCRpro::SHR* and End195 (**a** and **b**), *GL2pro::GUS* (**c** and **d**), or QC46 (**e** and **f**), either before (**a**, **c** and **e**) or after (**b**, **d** and **f**) SHR immunostaining. Arrows in **c** and **d** indicate presence of SHR protein in a cell of the outermost layer that normally should express *GL2*, and triangles point to both ends of an underlying cell. Abbreviations as in Fig. 1. Scale bars, 50 μm.

supernumerary cells having endodermal characters, the End195 GUS stain was found in all cells between the stele and the outermost layer (Fig. 3a). Immunolocalization of SHR on the same section showed a strong signal in the GUS-expressing cells, whereas staining was rarely detected in cells of the outermost layer (Fig. 3b).

In a similar analysis of the cross with the *GL2pro::GUS* line, GUS staining was detected only in cells of the outermost layer that were in contact with a single underlying cell (Fig. 3c). Contact with two underlying cortex cells is normally required for the acquisition of hair cell fate, and *GL2* is specifically expressed in the non-hair epidermal cells[12]. *GL2* expression in the *SCRpro::SHR* background is therefore analogous to wild type, indicating that the underlying cells need not be cortex for correct specification to occur. Occasionally we found cells in the outermost layer in which there was no GUS staining even though they were situated over a single underlying cell (Fig. 3c, arrow). The SHR immunostain revealed the presence of SHR protein in these cells (Fig. 3d, arrow). These results indicate that when SHR is found in cells of the outermost layer it is sufficient to alter their cell fate.

In the analysis of the cross with the QC46 line, the GUS stain was found in the 3–4 cell layers that extend toward the root cap from the base of the vascular cylinder (Fig. 3e). Immunostaining of this section revealed the presence of the SHR protein in all of the GUS-expressing layers (Fig. 3f), suggesting that production of multiple QC layers was a result of SHR in these cells. The formation of multiple QC layers should give rise to multiple layers of endodermis/cortex initial cells immediately adjacent to them. This idea is based on laser ablation experiments that showed that QC cells have a role in maintaining the surrounding initial cells by repressing their differentiation[2]. Formation of the supernumerary endodermis layers is unlikely to result solely from the presence of the ectopic QC layers, however, because the number of supernumerary endodermis layers exceeds by more than twofold the number of QC layers.

To determine whether *SCR* is involved in production of the supernumerary layers, we analysed *SCR* transcription in the *SCRpro::SHR* lines. Previous analyses showed that levels of *SCR* RNA were sharply reduced in *shr* mutants, suggesting that *SHR* is required for full transcriptional activation of *SCR*[6]. Consistent with this model, we observed strong GFP fluorescence from the *SCRpro::GFP* marker in the supernumerary cell layers (Fig. 4a). The presence of SHR protein correlated well with the GFP expression, as revealed by immunostaining of serial sections with either SHR or GFP antibodies (data not shown).

To determine whether SCR activity was necessary for the ectopic cell divisions in the *SCRpro::SHR* lines, we crossed a strong *SCRpro::SHR* line with the *scr-1* mutant, which has no detectable *SCR* RNA[7]. In plants carrying the *SCRpro::SHR* transgene and homozygous for the *scr-1* allele, the radial pattern was identical to that of the *scr* mutant (Fig. 4b). The progeny of a backcross to wild type had the *SCRpro::SHR* radial pattern, whereas all selfed F_3 progeny tested had the *scr* mutant radial pattern (data not shown). This shows that the lack of ectopic cell divisions in the *scr* background was not a consequence of inactivation of the transgene *per se*. In conclusion, the *SCRpro::SHR* phenotype requires a functional *SCR* gene, indicating that SHR activation of *SCR* is necessary for the longitudinal cell divisions that are essential for radial patterning.

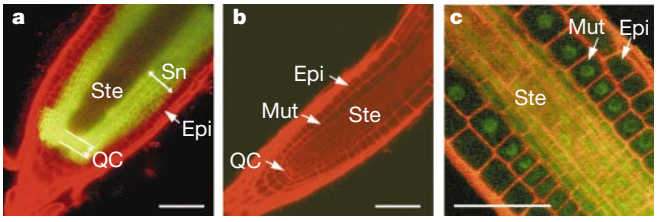

Figure 4 SCR acts downstream of SHR. **a**, *SCRpro::GFP* marker expression in a *SCRpro::SHR* transgenic root. **b**, Root phenotype of a *SCRpro::SHR* transgenic in the homozygous *scr-1* mutant background is the same as the *scr-1* phenotype. **c**, Expression of the SHR::GFP transgene in the homozygous *scr-1* mutant background results in detectable GFP fluorescence in the nuclei of the mutant layer. Mut, mutant layer. Other abbreviations as in Figs 1 and 2. Scale bars, 50 μm.

Although the longitudinal division of the cortex/endodermal initial daughter does not take place in *scr* mutants, the resulting single mutant cell layer has differentiated attributes of both cortex and endodermis[7]. To determine whether SHR protein can still translocate to the single mutant tissue layer, we crossed the SHR::GFP fusion protein line to the *scr-1* mutant. In plants carrying the SHR::GFP transgene and homozygous for the *scr-1* allele, GFP fluorescence was clearly visible in the nuclei of the mutant layer (Fig. 4c). We conclude that SHR protein movement and nuclear localization do not require SCR activity.

Movement of SHR protein provides a simple model to explain the non-cell-autonomous function of *SHR* required for root radial patterning. In this hypothesis, SHR has three functions: transmission of positional information through its own movement; activation of *SCR*; and cell-fate specification (Supplementary Information Fig. 3). The last two functions would require movement of SHR protein. To test this model, we enlarged the SHR-expression domain and analysed how well cell differentiation and activation of *SCR* correlated with localization of SHR protein. All the observed phenotypes can be explained by applying the model. In transgenic *SCRpro::SHR* plants, activation of *SCR* by SHR results in *in situ* production of SHR in the adjacent layer, because the SHR coding region is under control of the *SCR* promoter. This creates an autocatalytic reinforcement process of SHR signalling. The consequences of this reinforcement are SCR-dependent cell division and replacement of cortex (and occasionally epidermis) cell fate with endodermis cell fate, which is mediated by the cell-fate specification function of SHR. The ectopic presence of SHR in the outer daughter cell could be due to influx of the SHR produced from the *SCRpro::SHR* transgene in the inner daughter cell, or to *de novo* transcription from the transgene in the outer daughter cell mediated by the residual SHR, or to a combination of both. In the cells immediately below the stele, the reinforcement process and cell-fate specification result in multiple layers of QC. This indicates that cell-fate specification by SHR requires yet unidentified positional cues that are not mediated by SHR, because the presence of SHR can result in different fates when cells are in different positions.

Although our study does not address the pathway of SHR movement, previous work suggests that movement is likely to be through plasmodesmata[14]. In the shoot meristem, intercellular trafficking of transcription factors has been reported for structurally unrelated proteins[15,16]. The biological relevance of this movement is not evident because in wild-type plants these proteins are found in an identical domain as their cognate RNA. The one exception, the maize KNOTTED1 (KN1) homeobox protein has been reported to move to the outermost layer of the shoot meristem where its RNA was not detected[17]. But there is no evidence that protein presence in the outermost layer is essential for KN1 activity. In contrast, because the non-cell-autonomous activity of SHR is essential for patterning the adjacent cell layer, movement of SHR protein seems to have an integral role in root radial pattern formation.

In summary, we have shown that SHR protein can move and its translocation provides a simple model for its non-cell-autonomous activity in root radial patterning. Nuclear localization of SHR in the adjacent layer and activation of *SCR* strongly suggest that SHR is directly involved in transcriptional regulation in these cells. This simple strategy, which uses a single protein for both positional signalling and cell-fate determination, may have been important in the evolution of land plants to acquire efficient vascular function by forming radially organized tissues. □

Methods

Plasmid construction and plant transformation

To generate an in-frame fusion of SHR and GFP, we introduced restriction sites at both ends of the coding sequences for SHR and mGFP4 (with an S65T mutation[18]). A linker sequence encoding Asp-Pro-Gly was inserted between SHR and GFP. The resulting DNA fragment was used to replace the coding region of a 4.1-kb *SHR* gene fragment (including the 2.5-kb 5′-upstream region) fused to the nopaline synthase 3′ region in the binary vector pBIN19. To make the *SCRpro::SHR* construct, we fused a 2.5-kb *SCR* 5′ region and the 1.6-kb SHR coding region in the pBIH vector, which had been modified from pBIN19 to confer hygromycin resistance. The plasmids were electroporated into *Agrobacterium* strain GV3-101, which then was used to transform *Arabidopsis* plants by the floral dip method[19].

Marker analysis and microscopy

The Casparian strip, and JIM13 and CCRC-M2 antibody stains were performed as described[6]. We carried out JIM13 and CCRC-M2 antibody stains on the same section using appropriate secondary antibodies (rat and mouse, respectively). GFP fluorescence and propidium-iodide-stained cell walls in the root were observed by confocal microscopy as described[20]. Multi-photon microscopy was performed on a Bio-Rad MRC1024 MP multiphoton microscope equipped with a Coherent Mira 900-F infrared pulsed laser with operation wavelength of 935 nm. We carried out GUS staining as described[11]. Some microscopic images were processed with Photoshop (Adobe Systems) to increase contrast.

Antibody preparation

The SHR polypeptide lacking the amino-terminal 142 amino acids was expressed as a fusion protein to either thioredoxin (TRX::SHR) or maltose-binding protein (MBP::SHR) using pET32b (Novagen) and pET-MAL, respectively. pET-MAL was a hybrid plasmid made from pET40b (Novagen) and pMALc2x (New England Biolabs). We used TRX::SHR to raise antisera, and immobilized MBP::SHR on a gel matrix for affinity purification of the antisera. The proteins were induced in *Escherichia coli* strain BL21 (DE3). The insoluble TRX::SHR protein was solubilized with 8 M urea and purified with the HisBind Resin & Buffer Kit (Novagen). The purified TRX::SHR was dialysed, concentrated and injected into rabbits at Covance Research Products. The soluble MBP::SHR protein was affinity purified with Amylose Resin (New England Biolabs) and then coupled to NHS-activated Sepharose 4 Fast Flow (Amersham Pharmacia). In parallel, we extracted total soluble protein from the *shr-2* mutant roots and immobilized it on the Sepharose gel as above.

The antisera were diluted 10-fold in TBST buffer (20 mM Tris-HCl pH 7.5, 150 mM NaCl, 0.05% (v/v) Tween 20), and incubated with the MBP::SHR gel overnight with gentle agitation at 4 °C. The gel was washed once with TBST and once with CBST (50 mM sodium citrate pH 4.0, 150 mM NaCl, 0.05% (v/v) Tween 20). The bound antibodies were then eluted with GBST (50 mM glycine-HCl pH 2.5, 150 mM NaCl, 0.05% (v/v) Tween 20), and immediately neutralized by adding a 1/10 volume of 1 M Tris-HCl pH 7.5. This fraction was further absorbed to the *shr-2* protein gel for 7 h at 4 °C. The final unbound fraction was used for immunolocalization. Pre-immune serum purified in the same way showed no specific binding to wild-type root sections (data not shown).

Immunohistochemistry

Arabidopsis roots were fixed in 4% (w/v) paraformaldehyde in PBS (10 mM sodium phosphate pH 7.5, 130 mM NaCl) overnight at 4 °C, washed twice with PBS and embedded in 1% (w/v) agarose. The roots in excised agarose blocks were passed through an ethanol series followed by HemoDe (Fisher), and then embedded in Paraplast X-tra (Fisher). Sections (9 μm) were cut and placed on silane-coated slides (Polyscience). After dewaxing and rehydration, the sections were treated with HCl and proteinase K as described[16] with minor modifications (5 min in 0.2 N HCl and 10 min in 250 $\mu g\,ml^{-1}$ proteinase K). After blocking with TBST containing 1% (w/v) bovine serum albumin and 1% (v/v) goat serum for 4 h at room temperature, the sections were incubated with the purified anti-SHR antibodies (1/1,200 dilution relative to the antiserum) in the blocking solution overnight at room temperature. Slides were given six 10-min washes with TBST and incubated with alkali-phosphatase-conjugated anti-rabbit immunoglobulin-γ (1/1,000 dilution, Vector Lab) for 2 h at room temperature. After washing four times in TBST and twice in TBS (TBST lacking Tween 20), the signal was developed with NBT/BCIP (Roche Molecular Biochemicals) in 0.1 M Tris-HCl pH 9.5, 0.1 M NaCl, 1 mM levamisole for 2 h at room temperature.

Received 18 May; accepted 1 August 2001.

1. van den Berg, C., Willemsen, V., Hage, W., Weisbeek, P. & Scheres, B. Cell fate in the *Arabidopsis* root meristem determined by directional signalling. *Nature* **378,** 62–65 (1995).
2. van den Berg, C., Willemsen, V., Hendriks, G., Weisbeek, P. & Scheres, B. Short-range control of cell differentiation in the *Arabidopsis* root meristem. *Nature* **390,** 287–289 (1997).
3. Kidner, C., Sundaresan, V., Roberts, K. & Dolan, L. Clonal analysis of the *Arabidopsis* root confirms that position, not lineage, determines cell fate. *Planta* **211,** 191–199 (2000).
4. Dolan, L. *et al.* Cellular organisation of the *Arabidopsis thaliana* root. *Development* **119,** 71–84 (1993).
5. Benfey, P. N. *et al.* Root development in *Arabidopsis*: Four mutants with dramatically altered root morphogenesis. *Development* **119,** 57–70 (1993).
6. Helariutta, Y. *et al.* The *SHORT-ROOT* gene controls radial patterning of the *Arabidopsis* root through radial signaling. *Cell* **101,** 555–567 (2000).
7. Di Laurenzio, L. *et al.* The *SCARECROW* gene regulates an asymmetric cell division that is essential for generating the radial organization of the *Arabidopsis* root. *Cell* **86,** 423–433 (1996).
8. Knox, J. P., Linstead, P. J., King, J., Cooper, C. & Roberts, K. Pectin esterification is spatially regulated both within cell walls and between developing tissues of root apieces. *Planta* **181,** 512–521 (1990).
9. Freshour, G. *et al.* Developmental and tissue-specific structural alterations of the cell wall polysaccharides of *Arabidopsis thaliana* roots. *Plant Physiology* **110,** 1413–1429 (1996).
10. Esau, K. *Anatomy of Seed Plants* 215–242 (Wiley, New York, 1977).
11. Malamy, J. & Benfey, P. Organization and cell differentiation in lateral roots of *Arabidopsis thaliana*. *Development* **124,** 33–44 (1997).
12. Masucci, J. D. *et al.* The homeobox gene GLABRA2 is required for position-dependent cell differentiation in the root epidermis of *Arabidopsis thaliana*. *Development* **122,** 1253–1260 (1996).
13. Sabatini, S. *et al.* An auxin-dependent distal organizer of pattern and polarity in the *Arabidopsis* root. *Cell* **99,** 463–472 (1999).
14. Lucas, W. *et al.* Selective trafficking of KNOTTED1 homeodomain protein and its mRNA through plasmodesmata. *Science* **270,** 1980–1983 (1995).
15. Perbal, M., Haughn, G., Saedler, H. & Schwarz-Sommer, Z. Non-cell-autonomous function of the Antirrhinum floral homeotic proteins DEFICIENS and GLOBOSA is exerted by their polar cell-to-cell trafficking. *Development* **122,** 3433–3441 (1996).
16. Sessions, A., Yanofsky, M. F. & Weigel, D. Cell–cell signaling and movement by the floral transcription factors LEAFY and APETALA1. *Science* **287,** 419–421 (2000).
17. Jackson, D., Veit, B. & Hake, S. Expression of maize KNOTTED1 related homeobox genes in the shoot apical meristem predicts patterns of morphogenesis in the vegetative shoot. *Development* **120,** 405–413 (1994).
18. von Arnim, A. G., Deng, X.-W. & Stacey, M. G. Cloning vectors for the expression of green fluorescent protein fusion proteins in transgenic plants. *Gene* **221,** 35–43 (1998).
19. Clough, S. J. & Bent, A. F. Floral dip: A simplified method for *Agrobacterium*-mediated transformation of *Arabidopsis thaliana*. *Plant J.* **16,** 735–743 (1998).
20. Wysocka-Diller, J., Helariutta, Y., Fukaki, H., Malamy, J. & Benfey, P. Molecular analysis of SCARECROW function reveals a radial patterning mechanism common to root and shoot. *Development* **127,** 595–603 (2000).

Supplementary information is available on *Nature*'s World-Wide Web site (http://www.nature.com) or as paper copy from the London editorial office of *Nature*.

Acknowledgements

We thank K. Roberts for the JIM13 antibody; M. Hahn for the CCRC-M2 antibody; B. Scheres for the QC46 marker line; J. Schiefelbein for the GL2::GUS line; A. von Arnim for the GFP plasmid; M. Aida for the pBIH vector; and M. Starz for the assistance with confocal microscopy. Multi-photon confocal images were taken with assistance by J. Feijo and N. Moreno. K.N. was supported by a fellowship from Japan Society for the Promotion of Science. This work was supported by a grant to P.N.B. from the NIH.

Correspondence and requests for materials should be addressed to P.N.B. (e-mail: philip.benfey@nyu.edu).

Archipelago regulates Cyclin E levels in *Drosophila* and is mutated in human cancer cell lines

Kenneth H. Moberg, Daphne W. Bell, Doke C. R. Wahrer, Daniel A. Haber & Iswar K. Hariharan

Massachusetts General Hospital Cancer Center, Building 149, 13th Street, Charlestown, Massachusetts 02129, USA

During *Drosophila* development and mammalian embryogenesis, exit from the cell cycle is contingent on tightly controlled down-regulation of the activity of Cyclin E–Cdk2 complexes that normally promote the transition from G1 to S phase[1,2]. Although protein degradation has a crucial role in downregulating levels of Cyclin E, many of the proteins that function in degradation of Cyclin E have not been identified. In a screen for *Drosophila* mutants that display increased cell proliferation, we identified *archipelago*, a gene encoding a protein with an F-box and seven tandem WD (tryptophan-aspartic acid) repeats. Here we show that *archipelago* mutant cells have persistently elevated levels of Cyclin E protein without increased levels of *cyclin E* RNA. They are under-represented in G1 fractions and continue to proliferate when their wild-type neighbours become quiescent. The Archipelago protein binds directly to Cyclin E and probably targets it